3D Concrete Printing - Free Form Geometries with Improved Ductility and Strength

Zeeshan Ahmed(✉), Alessia Biffi, Lauri Hass, Freek Bos, and Theo Salet

Eindhoven University of Technology, Eindhoven, Netherlands
z.y.ahmed@tue.nl

Abstract. Additive manufacturing (AM) or 3D printing is a rapid prototyping process that has captured the attention of architects and designers worldwide in the last few years. Multiple research groups and commercial entities are exploring different areas of 3D concrete printing (3DCP) with one of the main topics being the potential to improve the design freedom, while simultaneously achieving sufficient structural ductility. Based on the target design impression of a free form 3DCP structure, this study presents a number of 3DCP strategies to print arbitrary double-curved geometries with improved concrete ductility. A digital design-to-fabrication workflow was applied, consisting of defining parameters at various stages of the process. Two case study objects have been printed, both featuring double-curved surfaces achieved through cantilevered printing with support material, and by printing on a curved support surface, respectively. The former object acted as support for the latter. Entrained cables and secondarily added glass fibres were used to obtain ductility. The result is a double-curved 1×1 m panel with fibre-reinforced printed concrete, as well as a double curved print bed, reinforced with high strength steel cables.

Keywords: Fabrication and robotics craft · Robotic production · 3D concrete printing

1 Introduction

Additive manufacturing (AM) or 3D printing is a rapid prototyping process that has captured the attention of architects and designers worldwide in the last few years. It has allowed designers and architects to realize digital designs into tangible objects (Bogue 2013). 3D printing has emerged as a truly disruptive technology of the 21st century which could drastically affect many manufacturing industries (Labonnote et al. 2016). The initial application of 3D printing in the field of architecture was for producing conceptual models to study design flaws and illustrating the final design models (Khoshnevis 1999). Today, the application of AM in architecture and construction has changed to manufacturing structural and non-structural elements by printing with concrete, steel, and other building materials.

© RILEM 2020
F. P. Bos et al. (Eds.): DC 2020, RILEM Bookseries 28, pp. 741–756, 2020.
https://doi.org/10.1007/978-3-030-49916-7_74

Concrete being cheap and readily available worldwide, with high strength, durability, fire-resistance and ability to be mould into any shape in its fluid state, makes it can an attractive material to apply for AM in construction. The most commonly adopted system for Additive Manufacturing of Concrete (AMoC) is based on an extrusion-type process, which was first developed by Khoshnevis and termed Contour Crafting (Khoshnevis 1999). Based on this approach, various research groups and start-up companies began to explore the degree of design freedom, as one of the potentials for the 3D concrete printing (3DCP) technology.

However, concrete as a material has its limitations, with a ratio of approximately 10:1, concrete has a relatively high compressive strength while being weak in tension. Furthermore, its failure behaviour can be characterized as brittle, i.e., without any meaningful plasticity. In conventional concrete structures, steel reinforcement bars are applied to overcome this issue, but this common strategy is generally not compatible with 3DCP processes. The application of 3DCP has been mainly limited to designs that are stressed only in compression (Salet et al. 2017). This restriction can only partially be overcome through strategies such as printing along stress lines as these stress lines still have to be compressive (Yongqiang and Chen 2010; Tam et al. 2016).

Another constraint of most current extrusion-based 3DCP processes is that, unlike standard desktop extrusion printers, they lack the option to apply temporary support structures that can be used to print cantilevering subsequent layers (i.e., layers not centrally stacked on each other). This limits the geometrical freedom significantly. Therefore, alternative approaches must be considered to improve the degree of design freedom for 3D printable objects.

2 Research Goal

To enhance the possibilities of extrusion-based 3DCP, strategies need to be devised that further increase the design freedom while simultaneously achieving sufficient ductility to achieve structural integrity. An arbitrary double-curved structure presented in Fig. 1 has been taken as a target application to showcase the generic nature of the strategy. This research aims to develop and apply 3DCP strategies that would allow its realization. A digital design-to-fabrication workflow was applied, consisting of defining parameters at various stages of the process.

Two case study objects were printed. In the first, a double-curved surface is achieved by printing cantilevering filaments that are supported during printing with a granular, temporary support material that can easily be added, removed and re-used. A previously developed method to entrain a reinforcement cable with the concrete filament was applied to obtain ductility (Bos et al. 2017). The second object, representing an actual part of the wall design, was printed on the double curved surface of the former. The print mortar was reinforced with fibres that were added to the mixture at the print head. The result is a double-curved 1×1 m panel, as well as a double curved print bed.

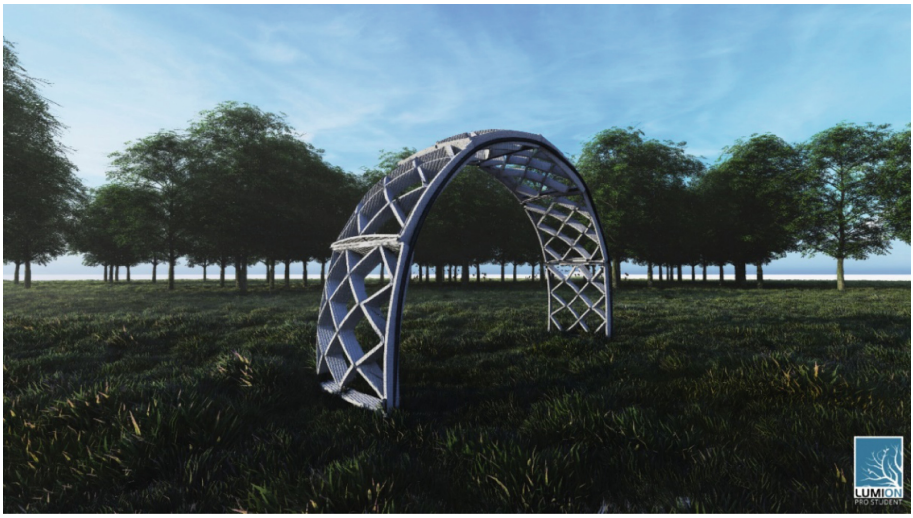

Fig. 1. Architectural concept design of a double-curved free-standing wall. Realization through 3DCP requires the development of a strategy both for the geometry and for the ductility.

3 Digital Workflow

A double-curved panel and its double-curved printed bed were designed using Grasshopper 3D, by following several design steps. The aim was to create a script that can automatically change the dimension of the print bed and the pattern of the panel depending on the required parameters for the panel, such as curvature angle, length, and width. The script also considers the requirements of the robot, such as the printed-element dimensions, the possible curvature angle printable using a gantry robot and the nozzle dimensions for the corner radius.

The script is composed of different parts. First, a double-curved surface was generated. For this specific experiment, it was generated by cutting a sphere (Fig. 2a), but also different double curved surface can be applied. The double-curved surface is characterized by a curvature angle of less than 20° (Fig. 2b). The limitation on the angle was based on the data from the previous printing experiments on double curve surface for printing the shell (Borg Costanzi et al. 2018). A higher inclination resulted in layers sliding off of each other or the print surface. The double-curved surface is then used as a starting surface to build the print bed. Secondly, the surface is extended towards a rectangular outer-perimeter (Fig. 2c). Following this procedure, a surface that corresponds to the target surface is obtained (Fig. 2d).

The 2D curved surface is made "printable" by transforming it into a 3D geometry. This is achieved by generating a box which base is the perimeter of the 2D curved surface. The resulting form is characterized by the upper side containing a double-curved surface (Fig. 3a) with the following dimensions: 1400 mm

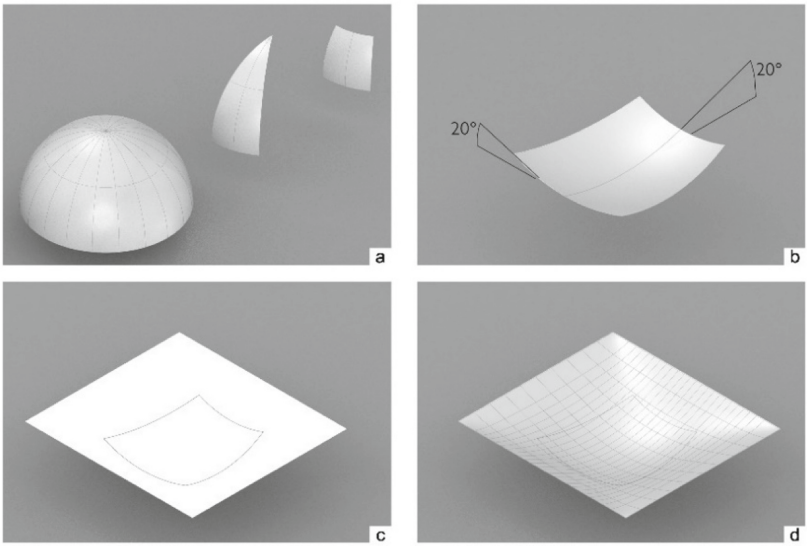

Fig. 2. (a) Development of the double-curved surface, which is generated by slicing a sphere's geometry. (b) The "sliced" surface from the sphere geometry, which is composed of a 20° curvature both vertically and horizontally. (c) Basic geometry used to create the surface of the print bed. (d) The boundaries of the double-curved shape and the rectangular perimeter create a double-curved mesh.

length × 1290 mm width × 400 mm height. To make the box 3D-printable, it is sliced into four pieces (Fig. 3b). To ensure the stability of the shape, an inner pattern is created. Lastly, the algorithm ensures that the corners of the shape have a minimum radius that is equal to the dimension of the nozzle (60 mm) (Fig. 3c) as a smaller radius results in excessive local material deposition.

A "woven" pattern was chosen for the double-curved surface as it allows the creation of an internal "net" within the design for both open and closed areas. Moreover, the "woven" pattern allows for multiple points of contact along the pattern, providing a more stable design (Fig. 3d).

The pattern was created by weaving together alternating points along the surface, which were extrapolated by the isocurve of the surface. An outer perimeter is added to the pattern that follows the outer edge of the panel, improving stability.

Figure 4 shows the centre-line of the print path. The minimum distance between two lines, to ensure contact between them, is equal to the nozzle width. The curvature radius of the pattern also corresponds to the dimensions of the nozzle. The final digital model of the geometries were sliced and converted to G-code using a Rhino Grasshopper based script to create toolpaths for printing.

4 Experimental Setup

The 3D concrete printing process adopted for this research is an extrusion-based process, which places filaments of concrete layer by layer with 4-degrees of freedom with a gantry robot, in a print area with a maximum size of $9 \times 4.5 \times 2.8$ m. It uses a 1-component dry mortar that is mixed with water and pumped to the print nozzle with an M-Tec Duomix 2000 mixer-pump through a 25.4 mm diameter rubber hose of 10 m length. The capabilities and limitations of the system have previously been extensively described (Bos et al. 2016).

For both objects, Weber 3D 145-2 mortar was used. The printability and hardened properties have been studied previously (Wolfs et al. 2018a; 2018b, 2019). In the support object, the standard water-to-dry mix ratio of 0.144 was applied. However, the water-to-dry mix ratio in the second printed façade panel object was 0.149, due to the use of fibres and the resultant workability loss.

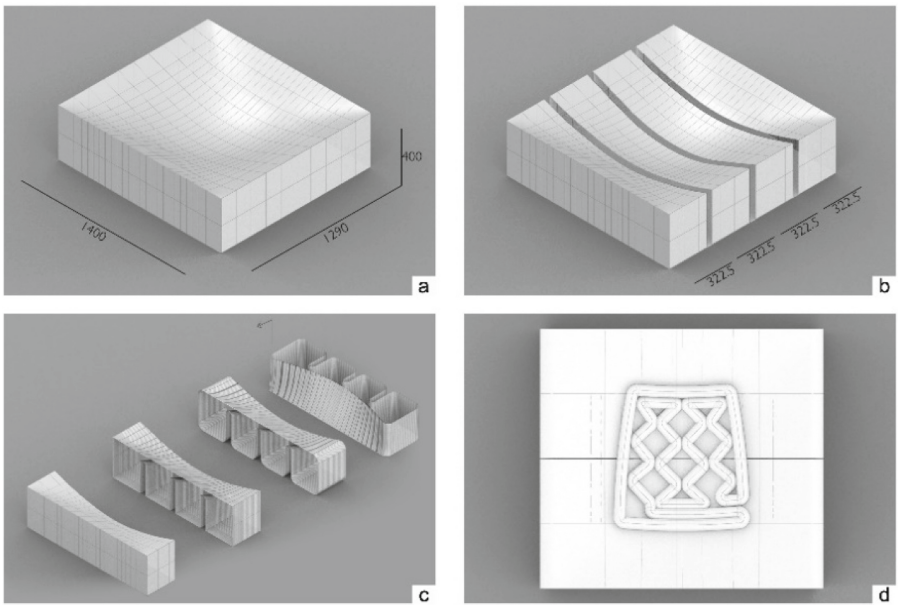

Fig. 3. (a) Dimensions of the print bed for the double-curved panel. (b) Subdivision of the print bed, so it can be 3D-printed. (c) Internal view of one section of the print bed. The internal pattern is created to provide more stability. (d) The double-curved surface is characterized by a "woven" pattern that ensures frequent areas of contact between the inner structure and the outer perimeter.

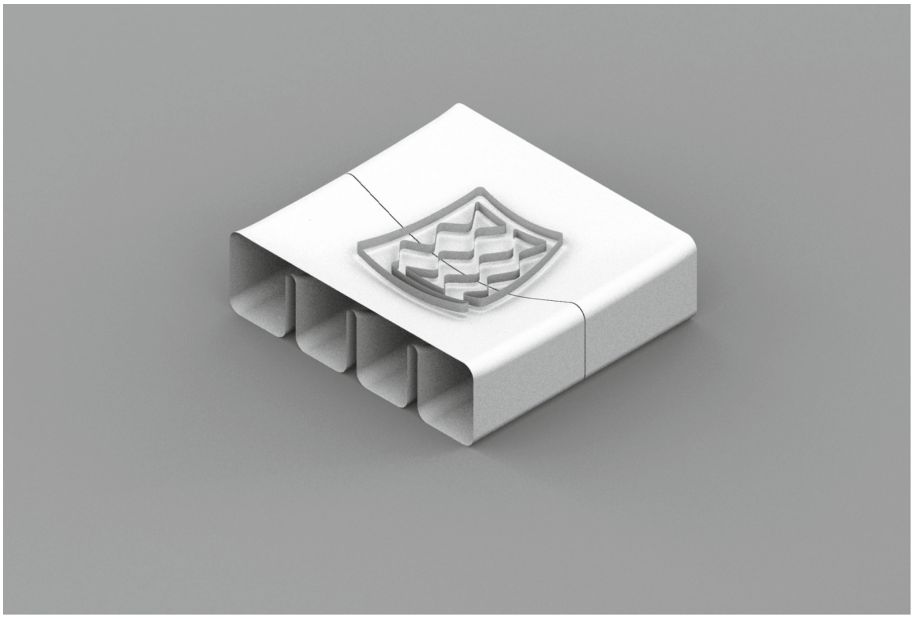

Fig. 4. The pattern's geometry has the same curvature as the print bed.

5 Strategies for Double Curvature

5.1 Printing with a Granular Support Material

To achieve design freedom for printing objects which can have a cantilever, experiments were conducted to develop a strategy to improve the bearing capacity of the support material without influencing the printed concrete. The first series of trial printings tests were performed to determine a suitable support material. To achieve this, different materials like kitchen salt (Fig. 5a), sand (Fig. 5b) and lightweight expanded glass aggregates (Fig. 5c) were explored. Based on availability and robustness, the lightweight expanded glass aggregates were finally used as the temporary support material.

Subsequently, an experiment was performed to establish the maximum achievable angle of cantilevering (Fig. 6). This was done by printing an arbitrary object of 453.3 mm height and 773.90 mm in diameter, with increasingly steep cantilevering angles (shown in Fig. 6b, the subsequent angles were 57.3°, 48.4°, 38.8°, and 21.9° with the horizontal). The object was printed with a 40 × 10 mm nozzle opening inside so that support material could be applied on both sides of the object. The experiment showed that the maximum cantilevering angle which could be achieved was approximately 30–40° (Fig. 6c) with lower angles the layers could not be adequately placed without affecting the bond between the layers (Fig. 6a).

Fig. 5. Example of supporting material: (a) Concrete printing with salt as supporting material (Retsin and Garcia 2016). (b) Sand as supporting material (Salet et al. 2017). (c) Lightweight granular aggregate.

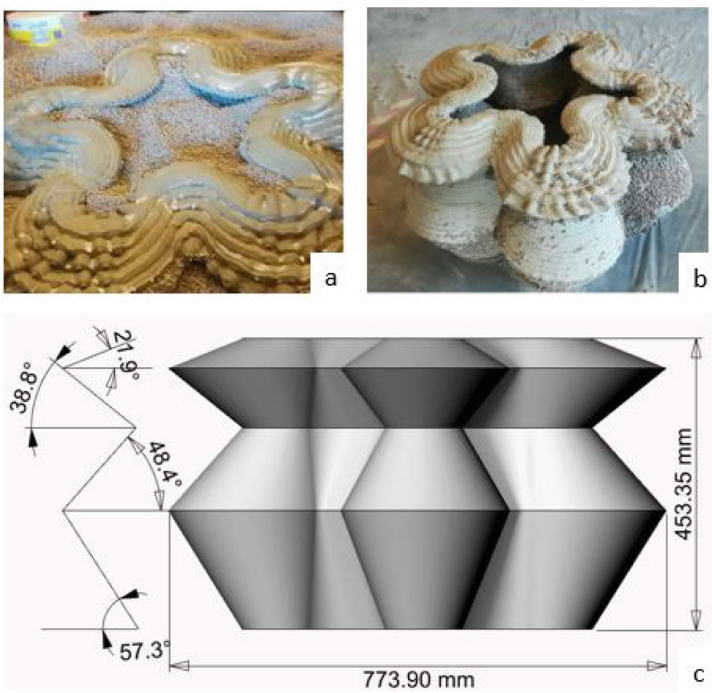

Fig. 6. Results from testing the support material.

A final print test focused on improving the system by printing without a confinement box. This was done by using the printed object itself to confine the supporting infill material. A conical object with 400 mm in height, 500 mm in bottom diameter and 250 mm in top diameter (cantilevering angle 64°) was printed without failure, thus validating the concept (Fig. 7).

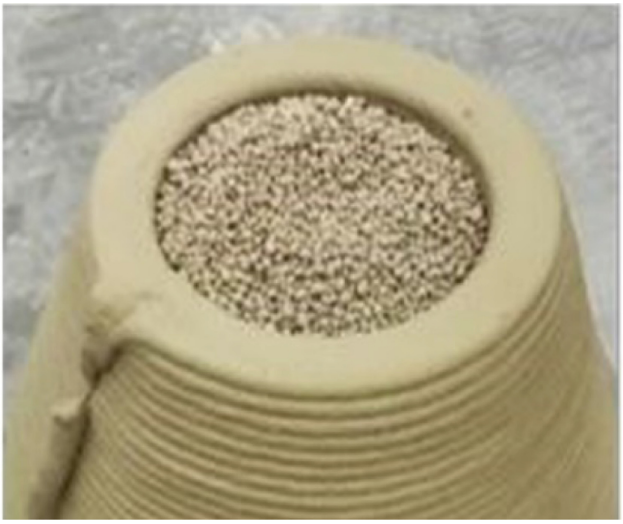

Fig. 7. Example of printing process without a confinement box.

5.2 Printing on a Double-Curved Surface

Increasing the form freedom of 3DCP by printing on a (double) curved surfaces has been previously performed (Borg Costanzi et al. 2018; Lim et al. 2016; Tam et al. 2016). Some of the issues to be considered, which have been identified in these studies include:

- The maximum angle of inclination before layers slide of the print surface or each other.
- The effects of a print nozzle not being perpendicular to the print surface due to a lack of sufficient DoFs of the robot.
- The localization of the print nozzle respective to the print surface.
- The material and fabrication of the print surface.

6 Strategies for Ductility

6.1 Reinforcement Cable

Currently, the problem of reinforcing digitally fabricated concrete has been recognized as one of the major issues to solve to allow a general breakthrough of these technologies (Salet et al. 2017). A range of different reinforcement strategies has been explored in academic studies and by commercial entities, as discussed to considerable extent by Asprone et al. (2018).

One of the strategies that have shown considerable potential is the automated entrainment of high strength steel cable in the concrete filament (Bos et al. 2017, 2018, 2020). A significant advantage is the fact that the cable can be applied concurrently with the deposition of concrete filament, i.e. no additional process steps are required. The potential of the concept has been confirmed by (Lim et al. 2016; Ma et al. 2019). In the current study, a Bekaert Syncrocord Force 0.6, with a diameter d = 0.63 mm and a yield load of 381 N has been applied in the first object (support object). It is extremely flexible, allowing it to follow the curved concrete filament. Even the 180 angles have been applied in the internal vertical supports in this object. The position of the reinforcement cable in the concrete is identical to the tool path (Fig. 10c).

6.2 Introduction of Fibres

Another strategy to obtain tensile strength and ductility in printed concrete is the addition of fibres to the matrix. Several researchers have explored this path, as shown in an overview by Wangler et al. (2019). An integration of 3D printing freeform complex geometries with fibre reinforced printed concrete has, to the knowledge of the authors, not yet been presented. The approach adopted in this research for introducing fibres into the printed concrete is through a simultaneous process of fibre deposition. A generic fibre reinforcement entrainment device (FRED) was used for introducing fibres into the printed layers, as shown in Fig. 8. Rather than incorporating fibres into the mortar before mixing in the mixer-pump, they have been added in a second step mixing unit at the print head. This method allows the use of a wider selection of fibres whereas the narrow cavities of the linear-displacement pump in the mixer-pump would only allow for very small fibres with limited structural effect. The detailed description of the device with the method of application has been elaborated in (Ahmed et al. 2020).

For this research glass fibres called CEM-FIL minibar 24 mm in length and a quantity of 58.9 kg/m^3 were used to improve the ductility of the printed panel. The double-curved façade element that was printed as the second object in this study was fibre reinforced. To determine the strength and ductility performance, a separate down-scaled Crack-Mouth Opening Displacement (CMOD) test was performed on the fibre reinforced material, according to the method previously described (Bos et al. 2019). The resulting CMOD-load diagram is shown in Fig. 9. With a residual strength ratio of approximately fR,3/fR,1 0.8 – 1, this combination is highly promising for structural applications even though further improvements in performance and production quality are required.

Fig. 8. Fibre reinforcement entrainment device (FRED) (Ahmed et al. 2020)

The double-curved façade element that was printed as the second object in this study was fibre reinforced. Rather than incorporating fibres into the mortar before mixing in the mixer-pump, they have been added in a second step mixing unit at the print head, through an innovative device that will be detailed in a future publication, and is based on a concept previously described (Bos et al. 2019). This method allows the use of a wider selection of fibres whereas the narrow cavities of the linear-displacement pump in the mixer-pump would only allow for very small fibres with limited structural effect. CEM-FIL 24 mm fibres (Owens Corning 2019) were applied, in a quantity of 58.9 kg/m^3. To determine the strength and ductility performance, a separate down-scaled Crack-Mouth Opening Displacement (CMOD) test was performed on the fibre reinforced material, according to the method previously described (Bos et al. 2019). The resulting CMOD-load diagram is shown in Fig. 9. With a residual strength ratio of approximately fR,3/fR,1 0.8 – 1, this combination is highly promising for structural applications even though further improvements in performance and production quality are required.

7 Printing Experiment

The final printing test consisted of two parts, each using a different strategy to achieve double curvature and ductility. The double-curvature was achieved through cantilevered printing with supporting material and ductility by the application of reinforcement cable. In the façade panel, double-curvature resulted from printing on the curved print-bed while ductility was achieved by applying fibres as described in Sect. 6.2.

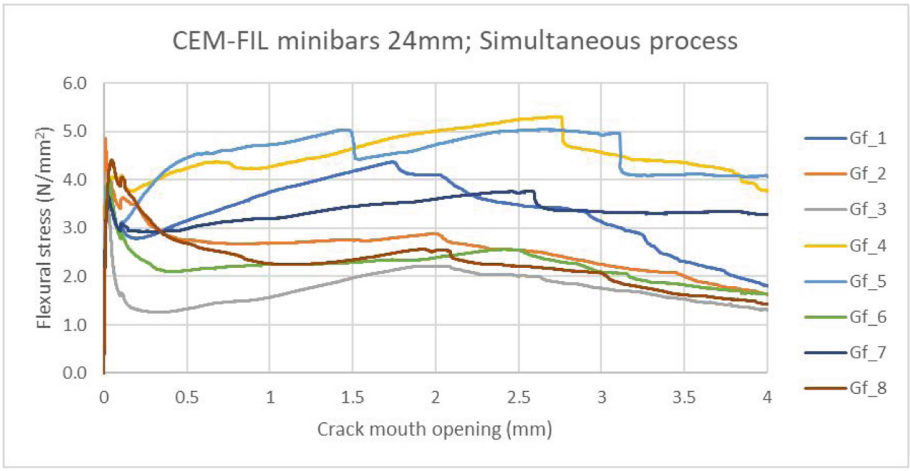

Fig. 9. Resulting CMOD-load diagram (Ahmed et al. 2020)

7.1 Double-Curved Support

The printed object was divided into four equal elements of 322 mm each along the width. This division was required because, since no containing box was used, outward cantilevering cannot be supported with the infill material, and, hence, the object must only cantilever inward during printing. A common failure mechanism in the fresh material state of 3DCP structures is buckling (Wolfs et al. 2018a; 2018b). However, since the interval for material deposition for consecutive layers is short, the object collapses during printing due to plastic failure (Fig. 10a).

Each element was printed and flipped by 90° before assembling (Fig. 10b) them as the printing process needs a flat print bed for supporting the deposited material. During assembling no additional material was used. The elements were leveled and placed next to each other.

The print nozzle used for this test was a hybrid-rectangular back/down flow nozzle with an opening dimension of 60×12 mm, as shown in Fig. 11. When reinforcement cable is used, the orientation of the flow of concrete filament requires particular attention. Research has shown that a vertical down flow results in the slicing of the filament by the cable while a horizontal backflow leads to a drastic reduction in layer adhesion (Salet et al. 2018).

To maintain a uniform layer dimension, the experiment was conducted with a print speed of 100 cm/s and an extrusion rate of 3.6 l/min. Layer offset between consecutive layers was 10.5 mm in height therefor each element comprised of 31 layers. Once the printing was completed, all the elements were sprayed with a curing agent (BMP Curing Compound AC) and wrapped with a plastic foil to avoid dehydration.

The experiment showed that the use of an infill material significantly improved the capabilities of 3DCP to print freeform geometries (Fig. 10c). Particularly for larger sized parts, the method is highly compatible with the use of automatically entrained reinforcement cables. However, the deposition of support material needs to be automated and synchronized with the deposition of the printed layers to be implementable in a large scale 3DCP application.

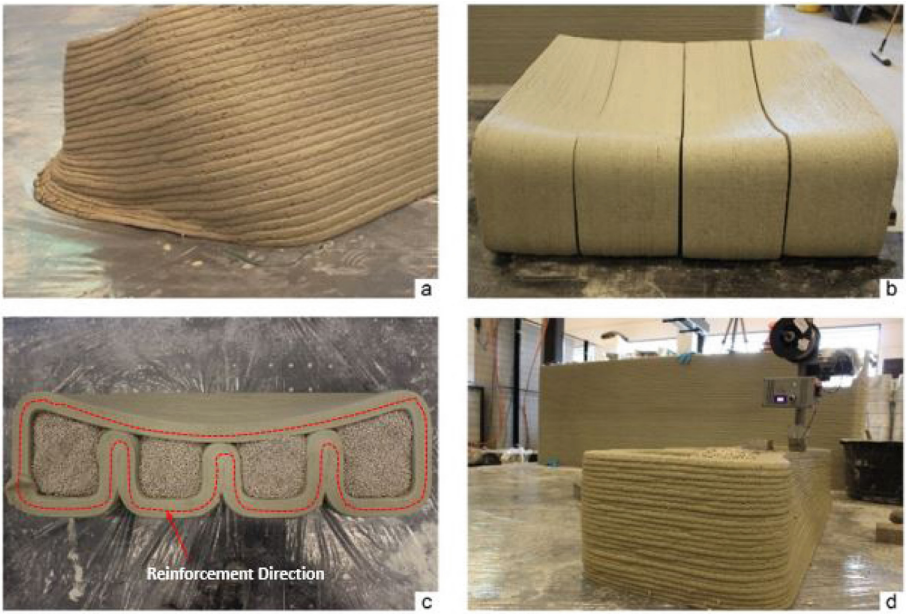

Fig. 10. (a) Effect of plastic failure during the printing process. (b) Subdivision of the print bed. (c) The inner pattern of the printed bed. (d) Reinforcement entrainment device (RED) during the printing process.

7.2 Double Curved Façade Panel

In the digital workflow for designing the print bed and panel, the dimension and curvature of the panel were based on the print bed and the overall base geometry from which it was generated. The other governing factor influencing the design considerations of the panel was mainly based on printing limitations. Due to considerations detailed in Sect. 3, the angle of the surface with the horizontal was limited to a maximum of 20°. Printing on a curved surface prohibited the use of reinforcement cable, as the required nozzle is geometrically incompatible with the curved surface. It should also be mentioned that a circular nozzle opening is easier to use on a double curved print bed (albeit not strictly necessary).

As the device used for fibre addition can be combined with any type of nozzle (rectangular, circular, down- or backflowing), a circular down flow nozzle

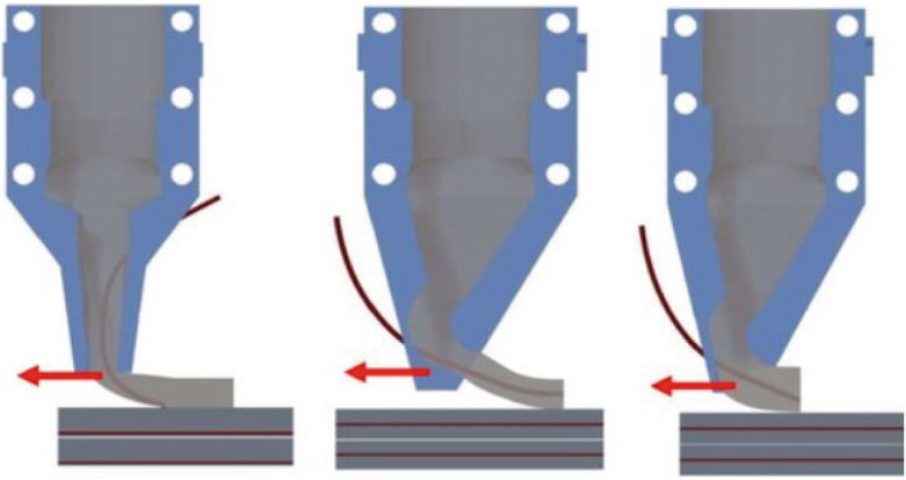

Fig. 11. Schematic showing the advantage for the hybrid nozzle for printing with cable reinforcement (Salet et al. 2018).

of 20 mm diameter was used. The print bed surface was covered with a foam sheet to obtain a smooth surface, covered with a plastic sheet to avoid the façade panel from adhering to the print bed.

Due to the smaller cross-section of the nozzle opening and the adjusted water-to-dry mix ratio (Sect. 4), the extrusion rate and the print speed needed to be re-synchronized. As a result, the print speed was increased to approximately 12 cm/s, and the extrusion rate was reduced to 2.8 l/min. As a circular nozzle was used to print the panel, the orientation of the nozzle was irrelevant. Thus, the rotational capacity of the print arm was not used. Due to the nozzle geometry, the allowable turning radius was also much smaller than for object 1, allowing for a more intricately designed panel (Fig. 12a). The layer offset for the initial layer was kept 10 mm from the curved print bed to produce layer dimensions of 40×10 mm. Similar to the printing of object 1, the panel was sprayed with a

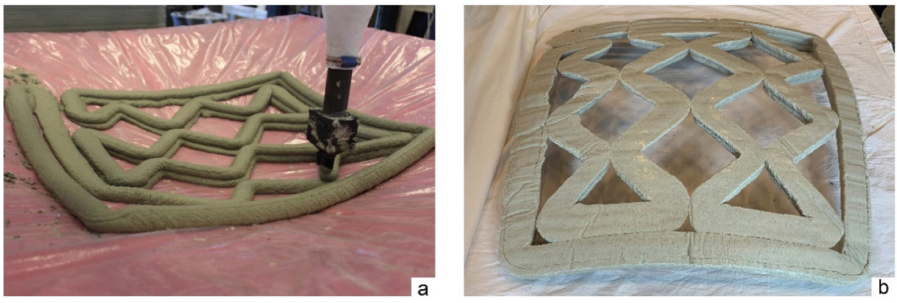

Fig. 12. (a) Printing inner geometry for the panel. (b) The final result of the double-curved panel.

curing agent (BMP Curing Compound AC) and wrapped with a plastic foil. It was allowed to cure and was left undisturbed in the print bed for 24 h before moving.

The printing process on the double curve print bed can be improved by printing with a 6-axis robotic arm as the nozzle can be always oriented perpendicular to the surface of the print bed (Fig. 13a) (Borg Costanzi et al. 2018). This could allow the use of reinforcement cable as well, which was not possible in the current experiment. However, printing on a curved surface is likely to stay limited to shell-type structures as increasing the number of layers will result in failure during printing due to the instability of the layers (Fig. 13b).

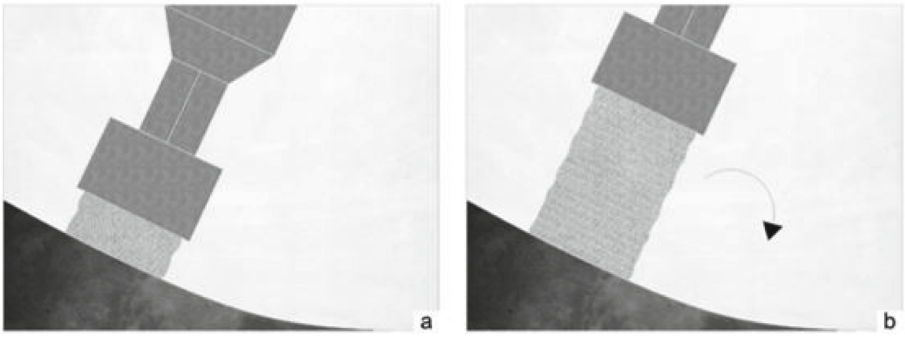

Fig. 13. (a) Printing using a 6-axis robotic arm, the material is placed perpendicular to the surface. (b) Failure during printing, due to the instability of the increasing number of layers.

8 Conclusions

Different strategies for achieving double curvature and ductility were used for both printed elements. Particular advantages of printing cantilevering layers with temporary support material and on a curved print bed were discussed. Their compatibility with the use of automatically entrained reinforcement cable and glass fibres were discussed. The resulting objects show that a double-curved 3D concrete printed structure is feasible through the use of the presented technologies.

Acknowledgements. The support of the staff of the Structures Laboratory Eindhoven is gratefully acknowledged. The support and guidance of Prof. ir. Juliette Bekkering, architect ir. Sjef van Hoof and, architect ir. Barbara Kuit is highly appreciated. The assistance in the 3DCP research of Master track students from Structural Design and graduation studio of Architectural Urban Design Engineering at the TU/e Department of the Built Environment is highly valued. For this paper, the authors appreciate the work of Remi Bogaert and Michael Yuen in particular, for their assistance in the experimental work. The TU/e research program on 3D Concrete Printing is co-funded by a partner group of enterprises and associations, that on the date of writing consisted

of (alphabetical order) Ballast Nedam, BAM Infraconsult bv, Bekaert, Concrete Valley, CRH, Cybe, Saint-Gobain Weber Beamix, SGS Intron, SKKB, Van Wijnen, Verhoeven Timmerfabriek, and Witteveen+Bos. Their support is gratefully acknowledged.

References

Ahmed, Z.Y., Bos, F.P., van Brunschot, M.C.A.J., Salet, T.A.M.: On-demand additive manufacturing of functionally graded concrete. Virtual Phys. Prototyping **15**, 1-17 (2020)

Domenico, A., Ferdinando, A., Costantino, M., Valentina, M.: 3D printing of reinforced concrete elements: technology and design approach. Constr. Build. Mater. **165**(2018), 218–231 (2018)

Domenico, A., Costantino, M., Bos Freek P., Salet Theo, A.M., Jaime, M.-F., Walter, K.: Rethinking reinforcement for digital fabrication with concrete. Cement and Concrete Research (2018)

Bogue, R.: 3D printing: the dawn of a new era in manufacturing? Assembly Autom. **33**(4), 307–311 (2013)

Bos, F.P., Dezaire, S., Ahmed, Z.Y., Hoekstra, A., Salet, T.A.M.: Bond of Reinforcement Cable in 3D Printed Concrete. in: Digit. Concr. 2020, 2nd RILEM Int. Conf. Concr. Digit. Fabr., 2020: p. Submitted

Freek, B., Zeeshan, A., Evgeniy, J., Theo, S.: Experimental exploration of metal cable as reinforcement in 3D printed concrete. Materials **10**(11), 1314 (2017)

Bos, F.P., Ahmed, Z.Y., Wolfs Rob, J.M., Salet Theo, A.M.: 3D printing concrete with reinforcement. In: High Tech Concrete: Where Technology and Engineering Meet, pp. 2484–2493. Springer, Cham (2018)

Freek, B., Rob, W., Zeeshan, A., Theo, S.: Additive manufacturing of concrete in construction: potentials and challenges of 3D concrete printing. Virtual Phys. Prototyping **11**(3), 209–225 (2016)

Bos, F.P., Bosco, E., Salet, T.A.M.: Ductility of 3D printed concrete reinforced with short straight steel fibers. Virtual Phys. Prototyping **14**(2), 160–174 (2019)

Borg, C.C., Ahmed, Z.Y., Schipper, H.R., Bos, F.P., Ulrich, K., Wolfs, R.J.M.: 3D Printing concrete on temporary surfaces: the design and fabrication of a concrete shell structure. Autom. Constr. **94**(2018), 395–404 (2018)

Norman, H., Viktor, L.W.: Mesh-mould: robotically fabricated spatial meshes as reinforced concrete formwork. Architectural Des. **84**(3), 44–53 (2014). http://dx.doi.org/10.1002/ad.1753

Huashangluhai. www.hstdgm.com. Accessed 14 May 2019

Khoshnevis, B.: Contour crafting-state of development. In: Solid Freeform Fabrication Proceedings, pp. 743-750. http://sffsymposium.engr.utexas.edu/Manuscripts/1999/1999-086-Khoshnevis.pdf. Accessed 27 July 2018

Nathalie, L., Anders, R., Bendik, M., Petra, R.: Additive construction: state-of-the-art, challenges and opportunities. Autom. Constr. **72**(2016), 347–366 (2016)

Yongqiang, L., Yong, C.: Beam structure optimization for additive manufacturing based on principal stress lines. Solid Freeform Fabrication Proceedings, pp. 666–678 (2010)

Sungwoo, L., Buswell, R.A., Valentine, P.J., Piker, D., Austin, S.A., De Kestelier, X.: Modelling curved-layered printing paths for fabricating large-scale construction components. Add. Manuf. **12**, 216–230 (2016)

Ena, L.F., Lex, R., Timothy, W., Fabio, G., Matthias, K., Flatt Robert, J.: Smart dynamic casting: slipforming with flexible formwork-inline measurement and control. HPC/CIC Tromsø 2017 (2017). Paper-no

Mechtcherine, V., Grafe, J., Nerella, V.N., Spaniol, E., Hertel, M., Füssel, U.: 3D-printed steel reinforcement for digital concrete construction-Manufacture, mechanical properties and bond behaviour. Constr. Build. Mater. **179**, 125–137 (2018)

Hiroki, O., Venkatesh, N., Viktor, M.: Developing and testing of strain-hardening cement-based composites (SHCC) in the context of 3D-printing. Materials **11**(8), 1375 (2018)

Owens Corning. http://www.ocvreinforcements.com. Accessed 19 May 2019. Pubnumber:10021900. Cem-FILMiniBars productsheet

Gilles, R., Garcia, M.Ji.: Discrete computational methods for robotic additive manufacturing: combinatorial toolpaths (2016)

Salet Theo, A.M., Ahmed Zeeshan, Y., Bos Freek, P., Laagland Hans, L.M.: Design of a 3D printed concrete bridge by testing. Virtual Phys. Prototyping **13**(3), 222–236 (2018)

Theo, S., Freek, B., Rob, W., Zeeshan, A.: 3D concrete printing– A structural engineering perspective. In: 2017 fib Symposium-High Tech Concrete: Where Technology and Engineering Meet. Springer International Publishing (2017)

Mark, T.K.-M., Mueller Caitlin, T., Coleman James, R., Fine Nicholas, W.: Stress line additive manufacturing (slam) for 2.5-d shells. J. Int. Assoc. Shell Spatial Struct. **57**(4), 249–259 (2016)

Weng, Y., Qian, S., He, L., Li, M., Tan, M.J.: 3D printable high performance fiber reinforced cementitious composites for large-scale printing (2018)

WinSun. http://www.winsun3d.com. Accessed 14 May 2019

Wangler, T., Roussel, N., Bos, F., Salet, T., Flatt, R.: Digital concrete: a review. Cem. Concr. Res. **123**, 105780 (2019). https://doi.org/10.1016/j.cemconres.2019.105780

Wolfs, R.J.M., Bos, F.P., Salet, T.A.M.: Early age mechanical behaviour of 3D printed concrete: numerical modelling and experimental testing. Cem. Concr. Res. **106**(2018), 103–116 (2018a)

Wolfs, R.J.M., Bos, F.P., Salet, T.A.M.: Correlation between destructive compression tests and non-destructive ultrasonic measurements on early age 3D printed concrete. Constr. Build. Mater. **181**, 447–454 (2018b). https://doi.org/10.1016/j.conbuildmat.2018.06.060

Wolfs, R.J.M., Bos, F.P., Salet, T.A.M.: Hardened properties of 3D printed concrete: the influence of process parameters on interlayer adhesion. Cem. Concrete Res. (2019). https://doi.org/10.1016/j.cemconres.2019.02.017.